Filtercake forming mechanisms at fracture and cavity openings

Problem presented by

F. F. Chang & M. Abbad

Schlumberger Carbonate Research Dhahran

Executive Summary

Oil wells can be stimulated to increase productivity by creating fractures and cavities in the sides of the bore hole which extend into the surrounding rock. These high-permeability channels are created by pumping *fracturing fluid* into the bore hole at high pressure, which can crack the rock. Once established most of the subsequent fluid flows out of the fractures as a result of their high permeability, thus inhibiting further cracking. This problem is resolved by injecting a *diverter fluid* containing particles and fibres, to plug the fractures temporarily and allow another cycle of fracturing fluid to stimulate a different region of the oil well. Finally the plugs, termed *filtercakes* are removed and oil production in the well commences.

In this report we investigate how the size and shape distributions, concentration, and material properties of particles and fibres in the diverter fluid affect the formation of the filtercakes. We consider how these properties may be engineered to maximize clogging in fractures and cavities, as near to the bore hole as possible, whilst minimizing the amount of material wasted.

The problem is approached by considering the two distinct aspects of the behaviour, namely the flow of particulates from the bore into the fracture, and the fracture clogging. A series of mathematical models are employed that elucidate the system behaviour, allowing us to offer guidance on the appropriate choice for the design parameters to optimize clogging.

Version 1.0
May 3, 2011
iii+16 pages

Report author

I. M. Griffiths & L. S. Gallimore

Contributors

M. Abdelaziz (KAUST)
S. Aseeri (KAUST)
C. J. W. Breward (U. of Oxford)
C. L. Farmer (U. of Oxford)
L. S. Gallimore (U. of Oxford)
I. M. Griffiths (U. of Oxford)
E. J. Hinch (U. of Cambridge)
J. R. Ockendon (U. of Oxford)
G. Olivier (KAUST)
K. C. Zygalakis (U. of Oxford)
V. Zubkov (U. of Oxford)

Contents

1 Introduction

Oil wells can be stimulated to increase productivity by creating fractures and cavities in the sides of the bore hole which extend into the surrounding rock. These high-permeability channels are created by pumping a fluid, termed fracturing fluid, into the bore hole at high pressure, which can crack the rock. This is followed by the injection of acid into the oil well, which further erodes and extends the fractures.

After such fractures have been established, their high permeability means most of the subsequent fracturing fluid flows through them and so inhibits cracking in other regions of the bore hole. To correct this a diverter fluid, typically a viscous fluid containing particles and fibres, is injected into the oil well to temporarily plug the fractures. This means that another cycle of fracturing fluid and acid injection can stimulate a different region of the oil well. A schematic diagram of this process is illustrated in figure 1. Finally the plugs, termed filtercakes are removed and oil production at the oil well commences.

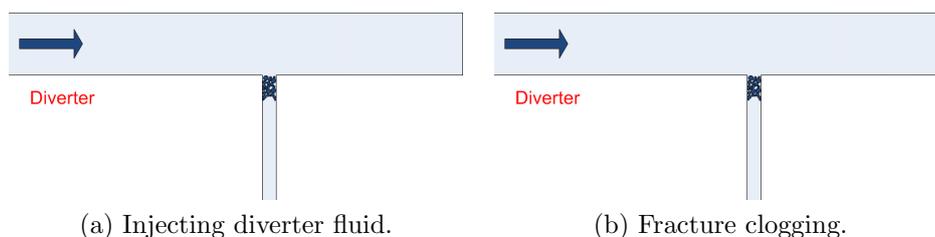
(a) Injecting diverter fluid. (b) Fracture clogging.

Figure 1: Diagrams showing how particles in the diverter fluid are injected into the bore hole, travel in the fluid and clog the highest permeability fracture.

Typical dimensions for the bore hole and fractures are given in figure 2.

2 Problem outline

The typical operational set-up comprises a bore with a series of fractured side channels, although the exact three-dimensional geometry of fractures along an oil well is specific to each oil well and changes over time. At any given time one of these fractures will have a greater permeability and will thus constitute the majority of fluid drainage from the bore. The goal of the design problem is simple and two-fold: to clog this channel by use of particles and fibres, which are injected at the bore entrance, with the minimum amount of diverter fluid. The blockage must be tough enough to withstand the subsequent injection of fracturing fluid (at a pressure of typically $100\,\mathrm{MPa}$) to allow the development of further fractures. Diverter material is considered wasted if it remains in the bore hole or flows down a high-permeability channel and is not used in clogging. It is important that this is minimized, because the clogging material must be removed before oil production can start, as well as being costly.

To minimize the quantity of particles and fibres injected before blockage is achieved we must first determine the motion of the particles in the main bore
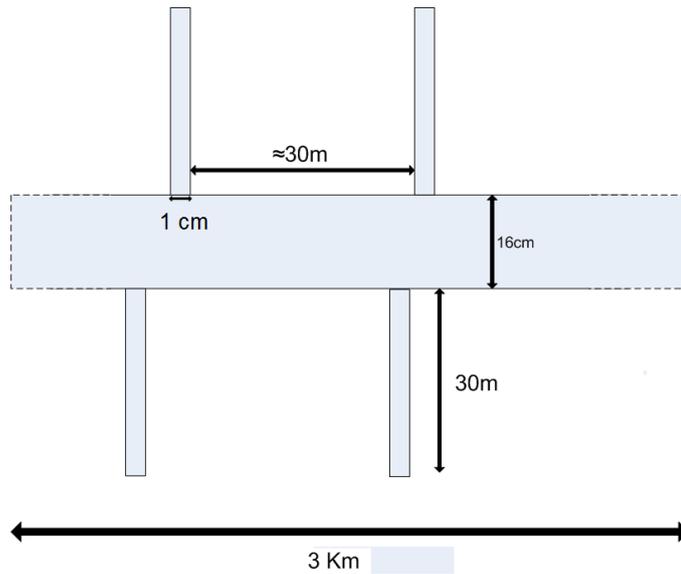
Figure 2: Typical dimensions for the bore hole.

channel. In particular we must maximize the quantity of particles injected that enter into the fracture. Once in the fracture, ensuring the blockage is tough enough to withstand the subsequent injection of fracturing fluid requires an understanding of the packing mechanism.

To satisfy the design criteria we have a series of parameters at our disposal. The simplest parameters are the freedom of particle size and shape, and the fibre length and flexibility. These are simple to adjust with no significant associated financial or practical penalty. The strategy for injection of these particulates provides a second aspect of flexibility. In particular, the velocity and concentration at which we inject the diverter fluid may be tuned to maximize clogging. A final feature that may be utilized is the particulate adhesiveness: both particles and fibres may be coated in a resin which aids in their coagulation and adhesion to the side walls of the fracture and it is anticipated that such a feature will enhance the clogging in the fracture.

In this report we investigate how the size and shape distributions, concentration, and material properties of particles and fibres in the diverter fluid affect the formation of the filtercakes. We consider how these properties may be engineered to maximize clogging in fractures and cavities, as near to the bore hole as possible, whilst minimizing the amount of material wasted.

We approach the problem by considering the two distinct aspects of the behaviour, namely the flow of particulates from the bore into the fracture, and the clogging of the fracture. We utilize a series of mathematical models to understand how the aforementioned design parameters may be chosen to optimize clogging. We conclude with recommendations to develop the work in this report further.

In table 1 we list typical operating parameter regimes for the process. This indicates that the Reynolds number,

$$Re = \frac{\rho_f u_f D_b}{\mu} \sim 10 - 10^4,$$

Fracturing fluid density	$\rho_f \sim 1000\,\mathrm{kg\,m^{-3}}$
Fracturing fluid viscosity	$\mu_f \sim 10^{-3}\,\mathrm{kg\,m^{-1}\,s^{-1}}$
Diverter fluid viscosity	$\mu_d \sim 1\,\mathrm{kg\,m^{-1}\,s^{-1}}$
Bore diameter	$D_b = 16\,\mathrm{cm}$
Fluid speed in bore	$u_b = 0.1\,\mathrm{ms^{-1}}$
Fracture width	$w_c \sim 1\,\mathrm{cm}$
Fluid speed in fracture	$u_c \approx 1.6\ \mathrm{ms^{-1}}$
Particle diameter	$d_p < 1\,\mathrm{mm}$
Fibre length	$L \sim 1\,\mathrm{cm}$
Fibre width	$w_f \sim 0.5\ \mathrm{mm}$
Fibre bending stiffness	$EI \sim 2 \times 10^{-4}\,\mathrm{Pa\,m^4}$

Table 1: Parameter values for operating regimes and associated nomenclature [1].

where $\mu_f \leq \mu \leq \mu_d$, and so the flow will remain laminar. Since all of the fluid is expected to flow out of the fracture, conservation of mass leads to the velocity in the fracture, $u_c = u_b D_b / w_c \approx 1.6\,\mathrm{ms^{-1}}$.

3 Mathematical modelling

3.1 Introduction

We begin by modelling the flow behaviour in the bore. As discussed in the Introduction, the specific geometry of the bore and fracture are unique to each operation, but all such processes are characterized by a common general geometrical framework, namely a main bore channel that is approximately 16 cm in diameter, with a fractured side channel of high permeability that is typically 1 cm wide, as illustrated in figure 2. As a result, the required insight for the behaviour is provided by considering the canonical problem of a main bore channel with a single perpendicular side channel. The geometry of this system mirrors the features that are fixed within the main problem, namely the bore and fracture dimensions. We consider the propagation of an initially fully developed parabolic flow as it approaches a fracture. We begin by focusing on the two-dimensional geometry and use this to extract conclusions on design recommendations, before generalizing to three dimensions.

In the original process the walls of the bore and the fractured channel are composed of rock and therefore effectively provide an impermeable barrier to the fluid. We thus impose zero fluid slip or penetration at each of these. As a consequence, before clogging, the fracture will accept the entire fluid injected at the entrance, which then drains through into the surrounding earth. This feature is captured within our model through the application of a constant pressure at the end of the fracture.

We note that the length of the fracture can extend up to 30 m, but for numerical expediency we choose a shorter length here. Additional simulations for extended geometries show no discernible difference in the behaviour near the entrance of the fracture where we are interested. Indeed, it is hoped that the diverter fluid induces
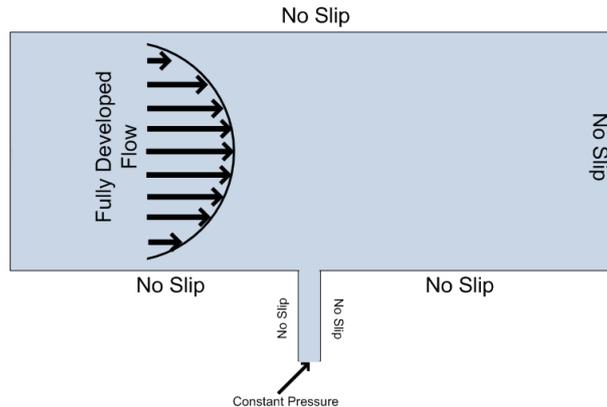
3

Figure 3: Canonical system geometry. We consider the steady solution of a fully developed parabolic flow profile approaching a fracture. No slip or penetration at the walls enforces the impermeability of the bore rock, while a constant pressure at the fracture outlet expresses seepage into the surrounding earth.

a blockage that extends no further than a few centimetres from the fracture inlet so the behaviour further down the fracture is not of practical interest here.

The final geometrical property presented in this system is the choice of the distance between the fracture and the end of the bore, and we investigate the effect this distance has on the flow behaviour in the subsequent section.

3.2 Modelling flow behaviour

We begin by modelling the steady-state flow behaviour observed in the absence of particles. The system is governed by the steady Navier–Stokes equations,

$$\boldsymbol{\nabla} \cdot \boldsymbol{u} = 0, \qquad \rho \left(\boldsymbol{u} \cdot \boldsymbol{\nabla} \boldsymbol{u} \right) = -\boldsymbol{\nabla} p + \mu \nabla^2 \boldsymbol{u},$$

where $\boldsymbol{u}$, ρ, p and μ denote the fluid velocity, density, pressure and viscosity respectively. We solve for the flow in the geometry and boundary conditions illustrated in figure 3 via a finite-element scheme, implemented in the numerical simulator Comsol. We use experimentally matched parameters with a Reynolds number, $Re = 100$.

The flow profile exhibits several notable features. Firstly, we notice that the flow out via the fracture induces circulation of fluid in the bore channel beyond the fracture (figure 4(a)). While conservation of mass enforces the flux of fluid out of the fracture to be equal to the flux at the entrance of the bore, it is apparent that there are areas of stagnation and recirculation beyond the fracture which will clearly play a key role in determining the motion of particles. While extending the distance between the fracture and the end of the bore is shown to generate more vortices, figure 4(b) shows that the flow behaviour near the channel is left qualitatively unchanged. We note that the fluid speed within each successive vortex falls rapidly so that the fluid is effectively stagnant as we move far to the right of the fracture.

4
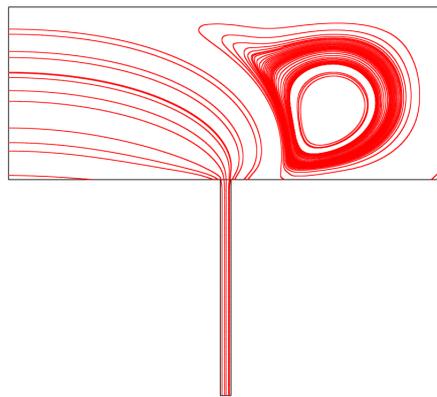
(a)
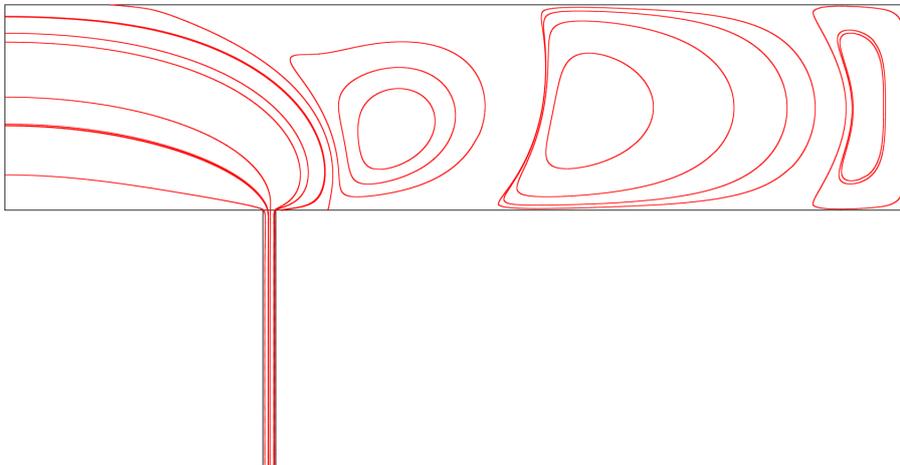
(b)

Figure 4: Diagram of streamlines in the flow for realistic parameters
($Re = 100$) and varying the distance between the fracture and the bore end.

3.3 Modelling particle trajectories

Having determined the motion of the fluid we progress to model the behaviour of the particles in the system. It is clear that a determining factor in the particle trajectories is the force experienced due to the fluid. Qualitatively, light particles will tend to follow the flow in regions where the direction of the fluid flow changes, while heavier particles will tend to follow their original path, taking longer to adjust to changes in flow direction. This feature is quantified through the particle Stokes number, given by [7]

$$St = \frac{\tau u}{d_c}, \tag{1}$$

where u is the flow speed, d_c is the characteristic dimension of the obstacle obstructing the fluid flow (chosen here to be the channel size), and τ is the particle response time; τ provides a measure of how long a particle takes to halt due to its inertia if we switch off the fluid flow, and is given by [11]

$$\tau = \frac{\rho_p d_p^2}{18\mu}, \tag{2}$$

where ρ_p and d_p are respectively the particle density and size. Substituting into (1) gives

$$St = \frac{\rho_p d_p^2 u}{18\mu d_c}. \tag{3}$$

Particles with a low Stokes number will tend to follow the flow streamlines as they change direction, while particles with a high Stokes number will tend to continue in the same direction despite changes in flow direction.

Rearranging (3) provides an expression for the diameter of a particle with unit Stokes number:

$$d_p = \sqrt{\frac{18\mu d_c}{\rho_p u}}. \tag{4}$$

For a particle flowing with speed $u = u_c$ in fracturing fluid, constructed from density-matched material ($\rho_p = 1000 \, \text{kg} \, \text{m}^{-3}$), $d_p \sim 0.3 \, \text{mm}$. This indicates that particles of less than 0.3 mm in diameter tend to follow the flow and enter the fracture. It is positive to find that such an estimate is in keeping with the proposed typical particle sizes. We utilize this observation in the simulations that follow. We note that we have chosen neutrally buoyant particles so that gravity does not affect their trajectories. If we chose particles with a different density to the fracturing fluid then clogging would also be dependent on the orientation of the fracture, a feature which could be exploited if the fracture orientation were known *a priori*. However, in general the well structure is arbitrary and so we should choose the diverter fluid must be chosen to penetrate cracks in all orientations optimally.

The specific particle trajectories are determined by modelling their behaviour under Khan–Richardson forces which express the force on a particle under viscous

conditions for a large dynamic range of Reynolds numbers (several orders of magnitude) [5],

$$\boldsymbol{F} = \frac{\pi d_p^2}{4} \rho |\boldsymbol{u}_f - \boldsymbol{u}_p| (\boldsymbol{u}_f - \boldsymbol{u}_p) \left(1.849 Re_p^{-0.31} + 0.293 Re_p^{0.06} \right)^{3.45}, \quad (5)$$

where $\boldsymbol{u}_f$ and $\boldsymbol{u}_p$ are the fluid and particle velocities, and $Re_p = \rho |\boldsymbol{u}_f - \boldsymbol{u}_p| d_p / \mu$ is the particle Reynolds number. Key to this analysis is that we assume the particles are suitably small so that they do not influence the flow, which we anticipate to be true in general in the real situation. Furthermore we assume that the particles are suitably disperse so that their motion does not influence each other. While the diverter fluid injected is expected to be fairly concentrated, we anticipate that the effects of Taylor dispersion [2, 10] will be sufficient to validate this assumption within the main flow.

We consider an initially uniform distribution of particles in the system at the inlet, and track their respective trajectories in the flow field calculated in § 3.2. As indicated by the discussion of the Stokes number, heavy particles are less amenable to the change in flow direction on the approach to the fracture and as a result, many of the particles pass the fracture to become entrained within the vortices past the channel. This is demonstrated explicitly in figure 5, where we show the trajectories for density-matched particles of size 1 mm (with a corresponding Stokes number $St \approx 10$) and size 0.1 mm (with a Stokes number of $St \approx 0.1$). This observation has an obvious impact on this problem since it highlights a fundamental, yet vital, design requirement: the particles must be suitably light so that they are able to change direction with the flow and be captured in the fracture. As we decrease the particle size we find that the number of particles captured increases as their ability to follow the streamlines increases. For extended geometries, the behaviour is qualitatively similar, as expected from the flow analysis shown in figure 4, with larger particles favouring entrainment in the vortices in the main channel, while smaller particles are more likely to be captured (figure 6).

However, it is evident that, to minimize the time and total number of particles used before clogging occurs, we need to choose particles that are as large as possible: it is intuitive that the larger the particles, the easier it will be to clog the fracture. Thus, since a greater proportion of smaller particles will flow into the fracture, but larger particles have a greater tendency to clog, we have therefore revealed an interesting optimization problem for the particle size.

3.4   The three-dimensional model

The analysis presented here may easily be generalized to the three dimensional system. In figure 7 we adopt a cylindrical representation for the bore with a rectangular side channel which replicates the actual fracture geometry. The behaviour exhibited is qualitatively similar to our two-dimensional geometries, namely that, as the particles are increased in the size they are observed to pass the fracture favouring entrainment within the vortices in the main bore channel. This simulation therefore justifies our two-dimensional simplification of the problem.
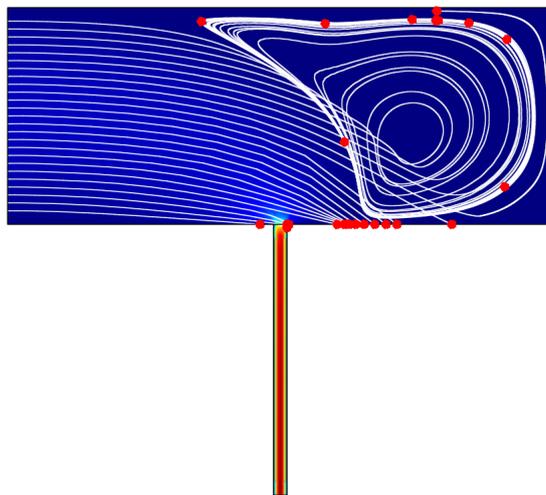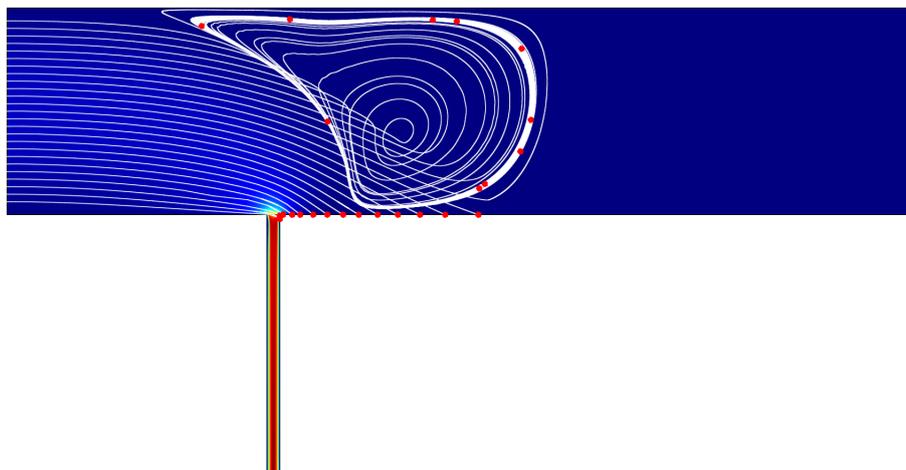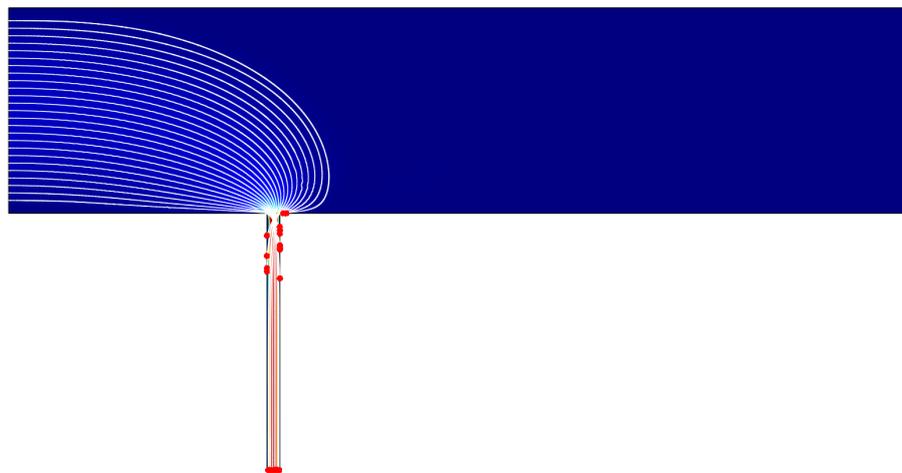
(a)
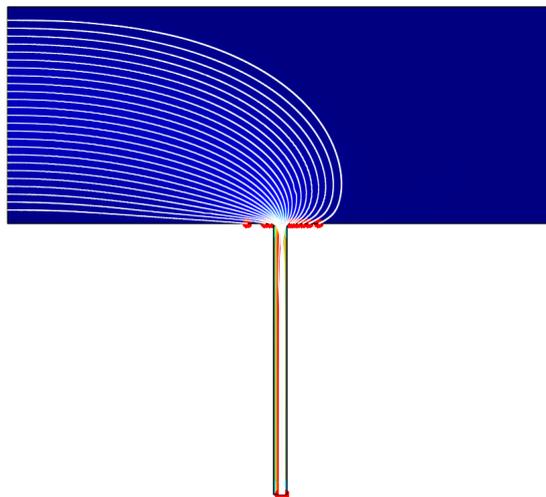
(b)

Figure 5: Particle tracing for the flow profile in figure 4, with $\rho_p = 1000$ and (a) $d_p = 1\,\text{mm}$ and (b) $d_p = 0.1\,\text{mm}$. The white lines depict the particle paths. We consider an initially uniform incoming particle distribution. The red dots show the final position of particles: due to the no-slip condition imposed at the wall we assume that once a particle strikes the wall it remains attached to the wall.

(a)

(b)

Figure 6: Particle tracing for the flow profile in figure 4, with $\rho_p = 1000$ and (a) $d_p = 1\,\text{mm}$ and (b) $d_p = 0.1\,\text{mm}$. The white lines depict the particle paths. We consider an initially uniform incoming particle distribution. The red dots show the final position of particles: due to the no-slip condition imposed at the wall we assume that once a particle strikes the wall it remains attached to the wall.
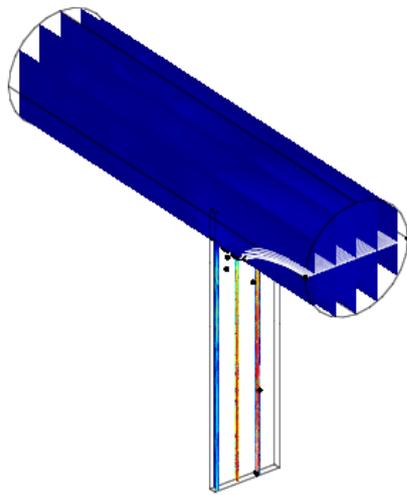
Figure 7: Particle tracing for a three-dimensional cylindrical bore geometry with a rectangular fracture, with $\rho_p = 1000$ and $d_p = 0.1\,\mathrm{mm}$. The white lines depict the particle paths, shown here for particles entering in the mid-plane of the bore channel.

3.5   Clogging in the crack

In this section we discuss strategies for optimizing particle clogging in the crack. As discussed in §3.3, it is evident from simple experiments that the channel will clog more easily when the particles are larger and when the rate of particle entry is higher. Specifically, the key parameter is the ratio of the mean cross-sectional area presented by the particulates in comparison to the total cross-sectional area of the fracture. We would typically require this ratio to be non-negligible (and as close to unity as possible) near the entry for clogging to occur in the absence of any adhesion. In addition, we would expect particles to align with the flow, orientating themselves in such a way as to present the minimum frontal cross-sectional. Consequently, the optimal choice for particle shape to minimize wasted material will be a sphere. It may be in some circumstances that non-spherical particles will fail to re-orientate themselves in time and thus present a larger cross-sectional area (see §3.6) but it is sensible to choose a contribution of the diverter fluid to contain spherical particles to ensure that at least some of the particles always present their maximum cross-sectional area.

Coating the particles with resin will promote coagulation between particles as well as adhesion to the sides of the bore and channel, and this will certainly aid in clogging. In figure 6(b) we notice that particles strike the right-hand edge of the crack. If the particles are adhesive this will allow them to stick to the wall and thus dramatically increase the likelihood of clogging. However, we recall that coagulation between particles in the main bore flow is undesirable since this will lead to larger particles that are less likely to be captured by the flow, instead favouring entrainment within the bore.

3.6   Fibre modelling

In this section we investigate the behaviour of fibres within the flow. The addition of fibres to a Newtonian liquid can dramatically alter the flow kinematics, and as a result, the orientation distribution has been a subject of extensive investigation both empirically and mathematically (see for example [4, 6, 9, 12]).

We begin by determining the compliance of the fibres, in particular whether we expect significant distortion of the fibres under the typical stresses exerted by the fluid. To model this we assume that upstream of the outlet the fibres align with the streamlines, which are approximately parallel to the walls. As the fibres approach the fracture a stress is exerted on the fibre due to the change in flow direction. For simplicity we approximate the flow on the fibre in the direction perpendicular to the channel, that is in the y-direction (see figure 8) by

$$v = -u_c \frac{x}{L}. \tag{6}$$

We note that we have chosen the velocity at the end of the fibre to be the maximum velocity in the fracture to ensure we obtain the maximal stress that can be felt by
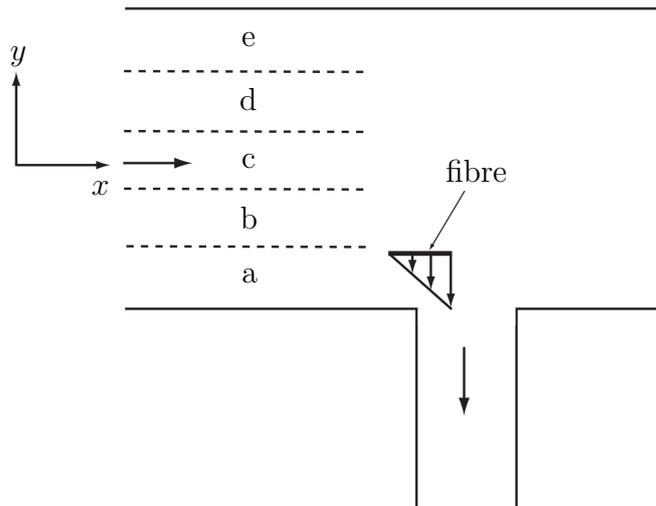
Figure 8: Schematic diagram for fibre motion near the hole. The position of the fibre in the bore is partitioned into five regions, a–e.

the fibre. The magnitude of the bending moment on the fibre is given by

$$M = \int_0^L \mu v x \, \mathrm{d}x = -\frac{\mu u_c L^2}{3}.$$ (7)

The magnitude of the curvature is then given by the expression

$$\kappa = \frac{|M|}{EI},$$ (8)

where EI is the bending stiffness of the fibre. Typical values from table 1 for a fibre in fracturing fluid yield $\kappa \sim 10^{-4}\,\mathrm{m^{-1}}$, and thus the curvature is extremely small. Consequently, this means that we can effectively model the fibres as rigid.

We may model the behaviour of a rigid fibre in a fluid using slender-body theory [3], which assumes that the disturbance motion of the slender body is approximately the same as that due to a line distribution of Stokeslets, that is, a singularity in Stokes flow representing the effect of a force applied to the fluid at a point. This theory provides a simplified system that permits a greater understanding of the fibre motion. While the application of this theory is for Stokes flow the predictions are valid for higher Reynolds number flows (see, for example [8]). The modelling approach adopted here closely follows the analysis of [8] and we refer the reader here for further details.

As the fibre approaches the junction, it will experience forces due to the fluid that cause both advection and rotation. As for the case of determining the particle trajectories in §3.3, to model the subsequent fibre motion in the flow, the flow field must be determined in advance (as calculated in § 3.2). Once known, slender-body

12

theory provides the equation for the motion of the fibres:

$$
\begin{aligned}
\boldsymbol{V} &= \boldsymbol{u}\left(\boldsymbol{x}_c + Ls\boldsymbol{p}\right) - \left(\boldsymbol{U} + \boldsymbol{\omega} \times Ls\boldsymbol{p}\right) \\
&= -2\left(-\log\left(\frac{\epsilon}{2}\right) + \log\left(\sqrt{1-s^2}\right)\right)(\boldsymbol{\delta} + \boldsymbol{pp}) \cdot \boldsymbol{f}(s) \\
&\quad - (\boldsymbol{\delta} - 3\boldsymbol{pp}) \cdot \boldsymbol{f}(s) - (\boldsymbol{\delta} + \boldsymbol{pp}) \cdot \int_{-1}^{1} \frac{\boldsymbol{f}(s) - \boldsymbol{f}(s')}{|s - s'|}\mathrm{d}s',
\end{aligned}
\tag{9}
$$

where $\boldsymbol{x}_c$ is the coordinate of the fibre mass centre, L is the fibre length, $-1 \le s \le 1$ parameterizes the distance along the fibre, $\boldsymbol{U}$ and $\boldsymbol{\omega}$ are the translational and angular velocity of the fibre respectively, $\boldsymbol{p}$ is the orientation vector, $\boldsymbol{\delta}$ the unit matrix and $\boldsymbol{f}(s)$ is the force on the fibre due to the fluid. Equation (9) provides $\boldsymbol{f}(s)$. Once determined, the total force and total moment on the fibre due to the flow are given respectively by

$$
\boldsymbol{F} = 4\pi\mu L \int_{-1}^{1} \boldsymbol{f}(s)\mathrm{d}s,
$$

$$
\boldsymbol{M} = 2\pi\mu L^2 \int_{-1}^{1} s\boldsymbol{p} \times \boldsymbol{f}(s)\,\mathrm{d}s.
$$

Newton's second law and the equation governing the fibre rotation then provide

$$
m\frac{\mathrm{d}\boldsymbol{u}}{\mathrm{d}t} = \boldsymbol{F}, \qquad\qquad \boldsymbol{J} \cdot \frac{\mathrm{d}\boldsymbol{\omega}}{\mathrm{d}t} + \boldsymbol{\omega} \times \boldsymbol{J} \cdot \boldsymbol{\omega} = \boldsymbol{M},
\tag{10a}
$$

where $\boldsymbol{J}$ is the moment of inertia, which may be used to determine the fibre trajectory. In figure 9 we show the typical change in angle as fibres of different sizes are drawn into the fracture. We observe that the fibres typically re-orientate themselves with the flow on a lengthscale of around ten centimetres. For the experimental set-up clogging is desired to occur within a few centimetres from the exit, suggesting that the fibres will not have fully re-orientated with the flow in this time. This is of significant importance to this problem since fibres that are not orientated with the flow offer a greater frontal area and thus an enhanced mechanism for clogging.

4 Conclusions

In this report we have considered a feasibility study for the formation of filtercakes as a mechanism for clogging of fractures for the industrial process of drilling an oil bore hole. The full problem statement was presented in the Introduction. Distillation of the key components of the problem from this description led to the study of the canonical fluid-dynamical problem for the flow out of a side channel.

Two distinct modelling aspects of this canonical problem were identified. Firstly the flow in the main bore determines the behaviour of particles, and, more specifically, the proportion of particles that are captured by the hole. Flow simulation and particle tracing yielded the first important conclusion, that if the particles chosen for the diverter fluid are too large they fail to be captured in the fracture, instead becoming entrained within the subsequent vortices in the main bore.
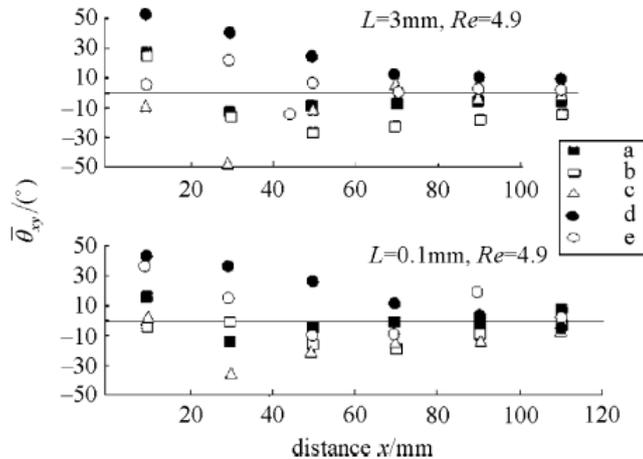
Figure 9: (a) Rotation of fibres of length 3 mm and 0.1 mm, with distance for $Re = 4.9$. The data points a–e refer to the different segments in the channel as shown in figure 8 and θ denotes the fibre angle relative to the wall [8].

The behaviour of a particle within a flow, specifically its tendency to follow changes in direction, is captured quantitatively by the particle Stokes number. This illustrated that, for the industrially relevant flow regime and parameters, particles with diameter that exceeds 0.3 mm should generally be avoided in order to ensure that they are captured by the fracture. We generalized these simulations to account for a more realistic three-dimensional geometry and found that this did not provide any marked additional insight, confirming that our two-dimensional approach captured the important behaviour of the problem.

The second modelling component to the problem concerned the behaviour of the particulates once within the fracture. In this problem it is the larger particles that are more desirable, that is (the converse of the requirement for particle capture) since this maximizes the chance for clogging. This presented an optimization problem in which, to ensure clogging occurs in the minimum time and with minimal particles we must ensure that the particles are small and light enough to be captured by the flow, but large enough so that clogging is favourable once the particulates enter the fracture. When placed in a flow, particles will tend to orientate themselves with the flow so that they present the minimum frontal cross-sectional area. Consequently, to maximize the chance of clogging for a given particle mass, the most suitable choice of shape is that of a sphere.

For our simulations we chose to use neutrally buoyant particles. Since the orientation of the fractures in a well is not a feature that is typically known, such particles provide the optimal choice for capture by an arbitrarily orientated fracture. If further information regarding the fracture orientation were known, changing the particle density may offer an additional level of control over clogging efficiency.

We then analysed the behaviour of fibres within the flow. We showed that the fibres used are effectively undeformed under the typical flow regimes. For typical operating conditions we showed that, during the process of being drawn into the

14

fracture, the fibres fail to re-orientate themselves with the flow. This improves the apparent frontal area of the fibres, and thus increases the chance of clogging. This allowed us to conclude that the use of fibres in addition to particles should provide an enhanced method for clogging and is a key part of the design choice for the diverter fluid.

We considered the importance of particle adhesiveness in the problem and found that by allowing the particles to stick to the walls and one another this led to an enhanced potential for clogging. However, under such circumstances, the aggregation of particulates within the main bore channel must be carefully controlled to ensure that coagulation is not significant enough to result in the particulates exceeding the maximum size criterion for particle capture before they have reached the fracture, so that they are still captured.

Finally, we discussed the strategy concerning the input for these particles. Simple experiments conducted to analyse the effect of the particle input rate on clogging clearly demonstrate that the rate at which particles enter must exceed a critical value for clogging to occur. This observation provides an insight into the most effective input strategy for a given total number of particles. Specifically, this suggests injecting the particles in a localized bolus rather than as a continuous stream to maximize their concentration and thus the chance of clogging when they reach the fracture. It is important that the input concentration choice takes into account the reduced concentration that will be seen downstream as a result of Taylor dispersion, which, for these flow rates, will be a significant effect.

We note that we did not consider the structural stability of the filtercakes once formed in this report. In particular, a key design requirement is that, once in place, these filtercakes must be able to withstand the $100\,\text{MPa}$ applied pressure of the subsequent injection of fracturing fluid. Modelling the strength of these filtercakes under pressure is therefore an important and extremely informative next step for the modelling undertaken here.

To conclude we offer a series of recommendations to develop the work undertaken here. Due to the highly experimental nature of this problem, the strongest path to take would be to conduct a series of small-scale laboratory experiments that replicate the key features of the system geometry and the problem. In particular, experiments that consider the effect of density on particle trajectories and their subsequent capture will be extremely important in validating the theories and the predictions made within this report. One aspect of the modelling that we did not consider was the exact adhesion and aggregation mechanism, and experiments to aid in understanding this would prove extremely useful. A further experiment to investigate the impact of Taylor dispersion within the main bore would also prove extremely beneficial in understanding the optimal strategy for particle injection at the inlet. Comparison of these experiments with the theories presented in this report should lead to an advanced understanding of the optimization of filtercake formation in the industrial set-up.

Bibliography

[1] Abbad, M. 2011 *Private communication.*

[2] Aris, R. 1956 On the dispersion of a solute in a fluid flowing through a tube *Proc. Roy. Soc.* **38**, 67–77.

[3] Batchelor, G. K. 1970 Slender-body theory for particles of arbitrary cross-section in Stokes flow. *J. Fluid Mech.* **44**, 419–440.

[4] Chiba, K., Yasuda, K. & Nakamura, K. 2001 Numerical solution of fiber suspension flow through a parallel plate channel by coupling flow field with fiber orientation distribution. *J. Non-Newtonian Fluid Mech.* **99**, 145–157.

[5] Coulson, J. M. & Richardson, J. F. 1999 Chemical Engineering Vol. 2, 5th Ed.

[6] Dong, S., Feng, X. & Salcudean M. 2003 Concentration of pulp fibers in 3D turbulent channel flow. *Int. J. Multiphase Flow* **29**, 1–21.

[7] Lee, S. S. 1999 Instrumentation for fluid-particle flow. *William Andrew Publishing.*

[8] Lin, J., Zhang S. & Olson, J. A. 2005 Numerical prediction of fiber motion in a branching channel flow of fiber suspensions. *Acta Mech. Sinica* **21**, 322–329.

[9] Lin, J. Z., Zhang,W. F., Yu, Z. S. 2004 Numerical research on the orientation distribution of fibers immersed in laminar and turbulent pipe flows. *Journal of Aerosol Science* **35**, 63–82.

[10] Taylor, G. I. 1953 Dispersion of soluble matter in solvent flowing slowly through a tube. *Proc. Roy. Soc. A,* **219**, 186–203.

[11] Wereley, S. T. & Nguyen, N.-T. 2002 Fundamentals and Applications of Microfluidics. *Artech House Publishers.*

[12] Yasuda, K. Mori, N. & Nakamura K. 2002 A new visualization technique for short fibers in a slit flow of fiber suspensions. *Int. J. Engineering Science* **40**, 1037–1052.